China Ocean Eng., Vol. 28, No. 3, pp. 317 – 330

DOI 10.1007/s13344-014-0026-3, ISSN 0890-5487

Wave Characteristics at the South Part of the Radial Sand Ridges of the Southern Yellow Sea

YANG Bin (杨 斌), FENG Wei-bing (冯卫兵)[1] and ZHANG Yu (张 俞)

College of Harbor, Coastal and Offshore Engineering, Hohai University, Nanjing 210098, China

(Received 19 April 2013; received revised form 9 October 2013; accepted 20 December 2013)

ABSTRACT

Based on one-year wave field data measured at the south part of the radial sand ridges of the Southern Yellow Sea, the wave statistical characteristics, wave spectrum and wave group properties are analyzed. The results show that the significant wave height ($H_{1/3}$) varies from 0.15 to 2.22 m with the average of 0.59 m and the mean wave period (T_{mean}) varies from 2.06 to 6.82 s with the average of 3.71 s. The percentage of single peak in the wave spectra is 88.6 during the measurement period, in which 36.3% of the waves are pure wind waves and the rest are young swells. The percentage with the significant wave height larger than 1 m is 12.4. The dominant wave directions in the study area are WNW, W, ESE, E and NW. The relationships among the characteristic wave heights, the characteristic wave periods, and the wave spectral parameters are identified. It is found that the tentative spectral model is suitable for the quantitative description of the wave spectrum in the study area, while the run lengths of the wave group estimated from the measured data are generally larger than those in other sea areas.

Key words: *wave characteristics*; *wave spectra*; *wave group*; *cold storms*; *radial sand ridges*; *Southern Yellow Sea*

1. Introduction

The study area is located at the south part of the unique radial sand ridges of the Jiangsu coast (the Southern Yellow Sea), where the nearshore bathymetry is very complicated (Fig. 1). In this area, the dominant wind direction is from north in winter and from south in summer (He *et al.*, 2010). The cold storms in winter and typhoons in summer are the main natural hazards to the coastal engineering (Jiangsu Province Resources Survey Leading Group Office, 1996). Furthermore, the local wave climate is also very complicated because of the unique bathymetry and the seasonal variation of winds. Therefore, it is essential to analyze the measured wave data in this area to gain the insight of the wave characteristics and to provide proper wave parameters for the coastal engineering design.

Recently many attentions have been paid to the wave statistics and the wave spectrum based on the field-measured data. Vandever *et al*. (2008) investigated the relationships between the wave height parameters and the spectrum width (ν) using data from acoustic Doppler wave gauges in ten different coastal and estuarine environments. Suh *et al*. (2010) explored the wave statistics in deep waters around Korean Peninsula based on various measured and hindcast data. They also analyzed the relationship between the significant wave height and the wave period, as well as the variability of the significant wave period, the spectral peak enhancement factor, and the directional spreading parameter. Kumar *et al*. (2010, 2011, 2012) studied the wave characteristics and spectrum under the influence of

1 Corresponding author. E-mail: wbfeng@hhu.edu.cn

summer monsoon along India coasts.

Around the Jiangsu coast, Gao (1995) studied the wind wave distribution and spectrum at Lvsi station, but due to the lack of sufficient data, the result is not enough to represent the research sea area. Feng *et al*. (2009) believed that there exists a good relationship between the wind speed and the wave height in the middle of the radial sand ridge area and the distribution of wave height is well consistent with that of Gluhovskii (1968). Feng *et al*. (2012) analyzed the unimodal spectrum of those waves with significant wave height larger than 0.7 m, and pointed out that the high frequency part of the wave spectrum decays with $f^{-4.24}$. They further proposed a tentative spectrum which agrees well with the measured spectrum.

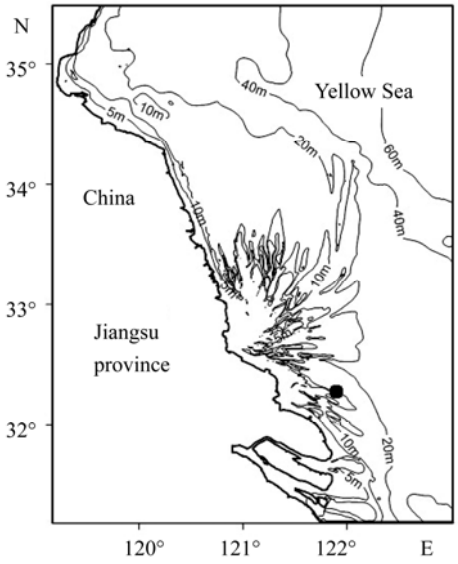

Fig. 1. Jiangsu coastal area and location of wave buoy '●' (32° 15.6043′N, 121° 58.5425′E).

Wave group is another important characteristic factor for the large waves. The low frequency response of coastal structures on the wave group is regarded as one of the main reasons for the structure destruction. For the first time, Ge (1986) has investigated the statistics of wave group at Lianyungang Port. Afterwards, Yu and Liu (1991) analyzed the wave group characteristics of Shijiu Port based on the wave envelope theory (Ewing, 1973), the statistical theory of runs (Goda, 1970) and the wave energy history method (Funke and Mansard, 1980). Kumar *et al*. (2003) studied the characteristics of wave group at four locations along the Indian Coasts using the statistical theory of runs (Goda, 1970).

In summary, although the previous studies provided valuable methods and information for wave statistics, wave spectrum and wave group, the systematic characteristics of waves in the study area are still unclear due to the lack of sufficient data. This study emphasizes on the studying of variations of wave characteristics, wave spectrum and wave group statistics at the south part of the radial sand ridges of Jiangsu coast. The results obtained in this study are useful for the design of coastal engineering, the operation of coast activities and the prediction of waves in the study area.

2. Wave Data and Method

2.1 Wave Data

The wave data used in this study were measured by a wave buoy from September 2008 to August 2009. The wave buoy is located at the south part of the radial sand ridges of Jiangsu coast, the Southern Yellow Sea (32° 15.6043′N, 121° 58.5425′E, as shown in Fig. 1). The water depth at the buoy location is around 10 m. The wave surface elevations were recorded at a frequency of 2 Hz for the duration of 17 min every 3 h. Before the analysis of wave parameters, wave records with H_{mean} smaller than 0.1 m were excluded to prevent the influence of transient waves.

2.2 Method

Firstly, zero up-crossing method is employed to calculate the wave characteristic parameters, including the significant wave height ($H_{1/3}$ or H_{s}), the significant period $T_{1/3}$, the mean wave period T_{mean}, the maximum wave height H_{max}, and the root-mean-square wave height H_{rms}.

Meanwhile, the Fast Fourier Transform method (FFT) is used to estimate the wave energy spectrum. The first obtained coarse spectrum is smoothed within the frequency domain with 34 degrees of freedom. The high-frequency cut off is set at 1 Hz with resolution of 0.0166 Hz. According to this smoothed wave spectrum, the wave spectral parameters are estimated, such as the significant wave height H_{m0}, the mean wave periods T_{m01} and T_{m02}, the spectral moments m_n $(n = 0, 1, 2, \cdots)$, the maximum spectral energy density S_{max}, the peak frequency f_{p}, the spectral peak parameter Q_{p} (Goda, 1970), the spectral width parameter ε (Cartwright and Longuet-Higgins, 1956) and the spectral width parameter ν (Longuet-Higgins, 1975). In addition, the regression analysis is applied to analyze the relationships, and the corresponding correlation coefficients between different parameters are calculated.

Finally, by using the statistical theory of runs, the run lengths of wave group are calculated by counting the number of consecutive waves exceeding a certain wave height. Definitions of the wave parameters used in the study are as follows:

$$H_{m0} = 4\sqrt{m_0}\ ; \tag{1}$$

$$T_{m01} = \frac{m_0}{m_1}\ ; \tag{2}$$

$$T_{m02} = \sqrt{\frac{m_0}{m_2}}\ ; \tag{3}$$

$$Q_{\text{p}} = \frac{2}{m_0^{\,2}} \int_0^{\infty} f S^2(f)\,\mathrm{d}f\ ; \tag{4}$$

$$\varepsilon = \sqrt{1 - \frac{m_2^{\,2}}{m_0 m_4}}\ ; \tag{5}$$

$$\nu = \sqrt{\frac{m_0 m_2}{m_1^2} - 1}; \tag{6}$$

$$m_n = \int_0^\infty f^n S(f) \mathrm{d}f; \quad n = 0, 1, 2, \cdots \tag{7}$$

where m_n is the n-th order spectral moment, f is the frequency, and $S(f)$ is the spectral energy density corresponding to f.

3. Results and Discussion

3.1 Variations of Wave Characteristic Parameters

Some of wave characteristic parameters from September 2008 to August 2009 are listed in Table 1. From Table 1, it can be seen that the significant wave height $H_{1/3}$ varies from 0.15 to 2.22 m with the average of 0.59 m, and the mean wave period T_{mean} changes from 2.06 to 6.82 s with the average of 3.71 s. The monthly average of significant wave height, the maximum wave height $H_{\max}$ and the maximum spectral energy density $S_{\max}$ in September 2008 and from November 2008 to March 2009 were higher than those of the other months. The spectral width parameter ε varies from 0.16 to 0.84 with the average of 0.55. The maximum wave height is 3.91 m occurred at 23:00 on December 21 from WNW direction, with the wave period of 5.41 s.

Table 1 Range and average of various wave characteristic parameters from September 2008 to August 2009

Month	$H_{1/3}$ (m)		$H_{\max}$ (m)		T_{mean} (s)		f_{p} (Hz)		ε		$S_{\max}$ (m^2/Hz)	
	Range	Average	Range	Average	Range	Average	Range	Average	Range	Average	Range	Average
9	0.18−1.97	0.66	0.32−3.52	1.10	2.33−5.89	3.78	0.08−0.45	0.20	0.29−0.75	0.58	0.02−7.32	0.50
10	0.15−1.36	0.52	0.23−2.19	0.87	2.36−5.82	3.59	0.12−0.48	0.23	0.24−0.74	0.54	0.01−2.38	0.27
11	0.15−1.84	0.66	0.23−3.31	1.10	2.06−6.23	3.68	0.07−0.51	0.22	0.18−0.82	0.55	0.01−3.73	0.50
12	0.17−2.22	0.73	0.27−3.91	1.22	2.13−6.13	3.70	0.07−0.48	0.22	0.16−0.81	0.55	0.01−7.06	0.67
1	0.16−1.94	0.57	0.25−3.48	0.97	2.21−5.59	3.66	0.12−0.50	0.22	0.22−0.73	0.54	0.01−4.24	0.47
2	0.16−1.80	0.69	0.25−3.34	1.14	2.10−5.56	4.02	0.12−0.50	0.19	0.18−0.78	0.59	0.02−5.56	0.56
3	0.16−1.89	0.67	0.25−3.25	1.09	2.29−6.07	4.01	0.10−0.45	0.20	0.21−0.79	0.58	0.01−4.22	0.50
4	0.17−1.74	0.58	0.28−2.52	0.96	2.15−5.68	3.58	0.12−0.50	0.23	0.17−0.76	0.53	0.01−4.79	0.41
5	0.15−1.39	0.45	0.27−2.49	0.76	2.16−5.72	3.40	0.08−0.50	0.24	0.20−0.84	0.51	0.01−2.14	0.21
6	0.19−1.19	0.51	0.32−2.31	0.84	2.25−6.82	3.76	0.07−0.47	0.22	0.22−0.82	0.55	0.02−1.86	0.27
7	0.15−1.21	0.52	0.23−1.89	0.86	2.17−6.40	3.84	0.07−0.48	0.21	0.19−0.80	0.57	0.01−1.49	0.26
8	0.18−1.59	0.54	0.27−2.42	0.91	2.33−4.87	3.47	0.12−0.48	0.23	0.28−0.71	0.52	0.01−1.56	0.27
Total	0.15−2.22	0.59	0.23−3.91	0.98	2.06−6.82	3.71	0.07−0.51	0.22	0.16−0.84	0.55	0.01−7.32	0.41

The occurrences of waves with different significant wave heights from September 2008 to August 2009 are presented in Table 2. It shows that the occurrence of waves with $H_{1/3} > 1$ m is about 12.4% of the total, among 5% occurred in the winter (from December to February of next year), 3.7%, 2.5% and 1.2% occurred in the summer, the autumn and the spring, respectively. The occurrences of waves with

$H_{1/3}$ > 1 m in September 2008, and November 2008 to March 2009 are larger than those in other months. The reasons for the large waves ($H_{1/3}$ > 1 m) in September 2008 are due to two typhoons (SINLAKU and JANGMI) passing through the East China Sea, which opens in the north to the Yellow Sea. And the large waves from November 2008 to March 2009 are mainly influenced by the cold storms.

Table 2 Occurrence frequency of the significant wave height of all levels from September 2008 to August 2009

$H_{1/3}$ range (m)	Month												Total
	9	10	11	12	1	2	3	4	5	6	7	8	
0.1−0.5	3.5%	4.5%	4.0%	3.4%	3.8%	3.2%	3.6%	3.7%	6.6%	5.6%	3.6%	2.7%	48.2%
0.5−1.0	4.2%	2.7%	3.5%	3.5%	1.2%	4.0%	4.9%	3.4%	2.9%	3.6%	3.4%	2.0%	39.5%
1.0−1.5	1.0%	0.5%	1.4%	1.6%	0.7%	1.5%	1.3%	0.6%	0.2%	0.5%	0.3%	0.4%	10.0%
>1.5	0.4%	0.0%	0.4%	0.6%	0.3%	0.3%	0.2%	0.2%	0.0%	0.0%	0.0%	0.0%	2.4%

The wave roses for occurrences of all waves and the waves with $H_{1/3}$ > 1 m from September 2008 to August 2009 are shown in Fig. 2. It shows that the dominant wave direction is in the SE direction with the occurrence frequency of 11.2%, and the other wave directions with high occurrence are ESE, WNW and SSE, which have the frequencies of 9.7%, 9.4% and 9.1%, respectively. For the waves with $H_{1/3}$ > 1 m, the wave direction distribution is not the same as that of all waves. The dominant wave direction is WNW with the occurrence frequency of 13.2%, and the other wave directions with high occurrence are W, ESE, E and NW, which have the frequencies of 11.6%, 10.6%, 9.9% and 9.6%, respectively. The small occurrence difference among those waves may be related to the complicated wind field in the study area. He *et al.* (2010) found that the wind field of the Jiangsu coast is complicated in different seasons. Furthermore, the wind field in different small part of the southern radial sand ridges is also different in one season. Therefore, the statistical results of the present study are reasonable.

Fig. 3 presents the wave roses of the occurrence frequency for waves with $H_{1/3}$ > 1 m in the four seasons from September 2008 to August 2009. It can be seen that the wave directions of high occurrence are WNW and E in the autumn, W and WNW in the winter, SE in the spring and SSW in the summer. The WNW direction has the highest occurrence, which is caused by the cold storms in the autumn and the winter.

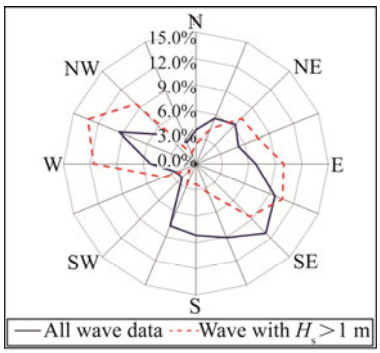

Fig. 2. Probability roses of the wave direction for all waves and waves with $H_{1/3}$ > 1 m.

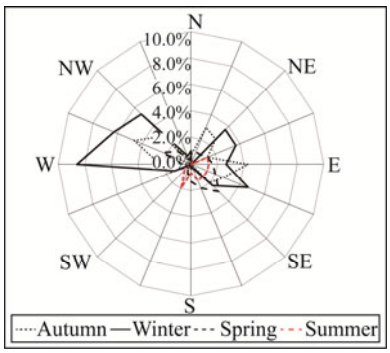

Fig. 3. Probability roses of wave direction for waves with $H_{1/3}$ > 1 m in different seasons.

3.2 Regression Analysis of Wave Parameters

3.2.1 *Wave Height*

The significant wave height $H_{1/3}$ is plotted against the maximum wave height H_{max} in Fig. 4. It can be clearly seen that the relationship between $H_{1/3}$ and H_{max} is very close with the correlation coefficient of 0.98. This study shows that the ratio of H_{max} to $H_{1/3}$ is 1.65 (ranging 1.31−2.52) by regression analysis, which equals the ratios along the Indian Coasts (Kumar *et al*., 2011). Theoretically, the value of $H_{max}/H_{1/3}$ is 1.53 (Longuet-Higgins, 1952), however Goda (1974) pointed out that the ratio is 1.8 as a guide for the design of vertical breakwaters. The present ratio lies somewhere in between.

Theoretically, the relationship between $H_{max}/H_{1/3(mode)}$ and N_0 is $H_{max}/H_{1/3(mode)}=0.706\sqrt{\ln(N_0)}$ (Longuet-Higgins, 1952). In the present study, $H_{max}/H_{1/3(mode)}$ is 0.96 times $0.706\sqrt{\ln(N_0)}$ by the linear fitting.

The theoretical definition of H_{m0} is $4.0\sqrt{m_0}$. Goda (1979) analyzed the field data and found that the ratio of wind waves in deep waters is 3.8 instead of 4.0. Moreover, in shallow waters (depth of 15 m), the ratio is 3.72 (Kumar *et al*., 2011). Fig. 5 shows the relationship between $H_{1/3}$ and $\sqrt{m_0}$ derived from the measured data. The significant wave height is $3.75\sqrt{m_0}$, which is smaller than the theoretical value. In addition, the values of $H_{1/10}/H_{1/3}$, $H_{1/3}/H_{mean}$ and H_{rms}/H_{mean} in this study area are 1.24, 1.54 and 1.11, respectively, which are smaller than the corresponding value 1.275, 1.598 and 1.128 based on the Rayleigh distribution theory (Longuet-Higgins, 1952). All these phenomena are mainly due to the shallow water effects.

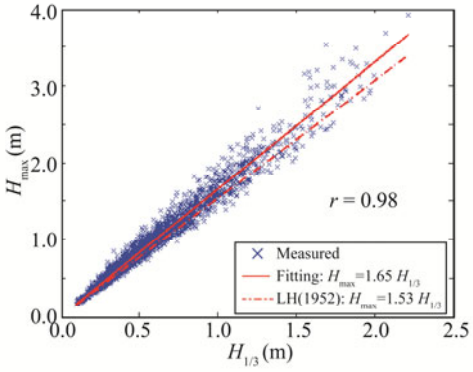

Fig. 4. Variation of H_{max} and $H_{1/3}$.

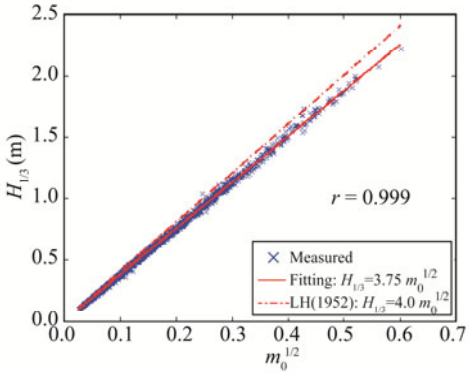

Fig. 5. Variation of $H_{1/3}$ and zeroth moment $\sqrt{m_0}$.

3.2.2 *Wave Period*

The wave period does not exhibit a universal distribution like the wave height. Thus, the ratios between the different characteristic wave periods, theoretically, are not always constant. Goda (2000) obtained the relations of $T_{max} \approx T_{1/10} \approx T_{1/3} \approx 1.2T_{mean}$ by analyzing the waves along Japanese coasts. In this study, the significant wave period $T_{1/3}$ is highly correlated to T_{m01}, T_{m02}, T_{mean} and $T_{1/10}$ with the

correlation coefficients of 0.986, 0.97, 0.97 and 0.99, respectively. $T_{1/3}$ is 1.12, 1.19, 1.17 and 0.99 times as long as T_{m01}, T_{m02}, T_{mean} and $T_{1/10}$ by the linear fitting, respectively. Figs. 6 and 7 show the variations of $T_{1/3}$ with T_{m01} and $T_{1/3}$ with T_{mean}, both with good linear fitted curves. Although the spectral peak period T_{p} has positive relationships with T_{m02} and $T_{1/3}$, and the linear relationships seem not very good between them (Figs. 8 and 9).

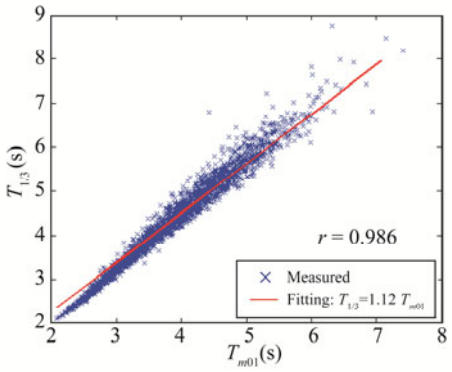

Fig. 6. Variation of $T_{1/3}$ with T_{m01}.

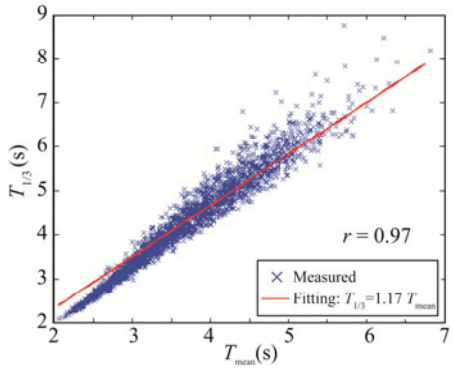

Fig. 7. Variation of $T_{1/3}$ with T_{mean}.

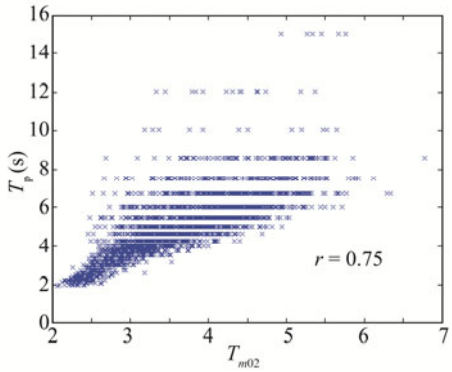

Fig. 8. Variation of T_{p} with T_{m02}.

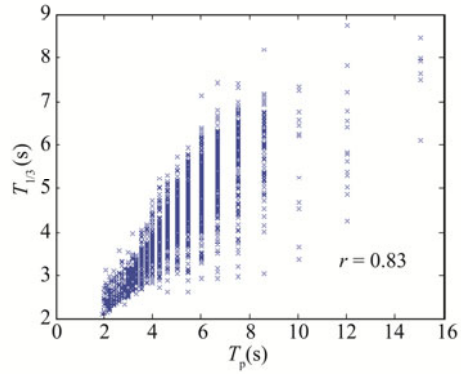

Fig. 9. Variation of $T_{1/3}$ with T_{p}.

3.2.3 *Wave Height and Wave Period*

More and more attention is paid to the relationship between the mean wave period T_{m02} and the significant wave height H_{m0}, and many empirical relations are proposed at different research areas. The relationship between T_{m02} and H_{m0} are $T_{m02}=5.4H_{m0}^{0.25}$ and $T_{m02}=5.03H_{m0}^{0.345}$ raised by Kumar *et al.* (2010, 2011), which obtained by analyzing wave data measured at the water depth of 14 m in Goa, which is located at the west of Indian Coast, and measured at the water depth of 15 m in the North Arabian sea (correlation coefficient of 0.72 for the latter). In this study, the relation between H_{m0} and T_{m02} for large waves (H_{m0} > 1 m) is $T_{m02}=3.97H_{m0}^{0.34}$ with the correlation coefficient of 0.53 (Fig. 10). For the same H_{m0}, the calculated result of T_{m02} is smaller than that of Kumar *et al.* (2010, 2011). The reason is that most of the wave spectra in this study are single-peaked, which are generated by winds, and most of wave periods are relatively small. However, the majority of wave spectra along Indian Coasts are multi-peaked, which are composed of swells with young sea, leading to relatively large wave periods.

In practical engineering applications, the relationship between the significant wave period $T_{1/3}$ and the corresponding wave height $H_{1/3}$ is also an important factor. Fig. 11 shows the variation of $T_{1/3}$ with $H_{1/3}$ for large waves ($H_{1/3}$ > 1 m), and the relation between $T_{1/3}$ and $H_{1/3}$ is $T_{1/3} = 4.89H_{1/3}^{0.41}$ (correlation coefficient of 0.59). Most of the measured points are above the empirical formula of $T_{1/3}=3.3H_{1/3}^{0.63}$ (Goda, 2003) and $T_{1/3}=3.85H_{1/3}^{0.5}$ (U. S. Army, 1977, Shore Protection Manual, abbreviated as SPM hereinafter). The reason is that the waves in this study area belong to the shallow water waves, and the large wave processes are limited by the water depth and the complicated submarine topography. However, the empirical formula of Goda and SPM are both derived based on the wave data measured in deep waters. Consequently, the derived relationship between $T_{1/3}$ and $H_{1/3}$ in this study leads the larger wave period than the other two empirical relationships for the same wave height do.

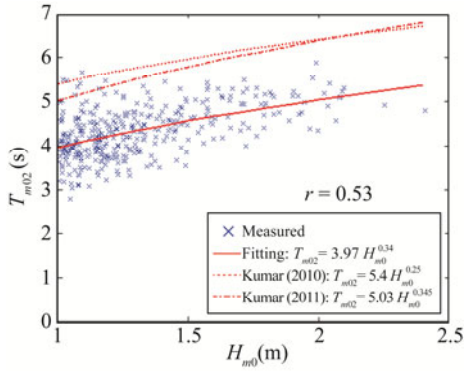

Fig. 10. Variation of T_{m02} with H_{m0}.

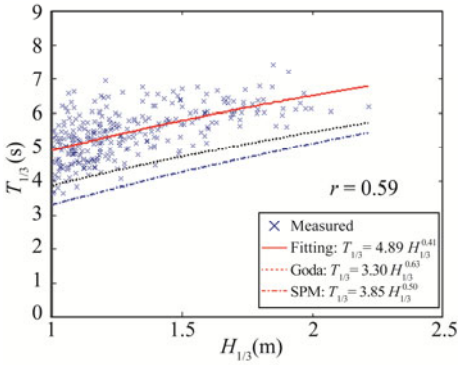

Fig. 11. Variation of $T_{1/3}$ with $H_{1/3}$.

3.3 Characteristics of Wave Spectra

3.3.1 *Statistics*

This study shows that the majority of wave spectra (88.6%) are single-peaked during the measurement period. These waves may be wind waves or swells, which can be identified by the method of Portilla *et al.* (2009). The identification result is shown in Table 3. It is illustrated that 36.3% of single-peaked waves are wind waves with high occurrence in the SE, SSE and WNW directions, and the rest are young swells with high occurrence in the WNW, ESE to SSW directions.

Table 3 Direction probability distribution of single-peaked wind waves and swells

Direction	Wind waves	Swells	Direction	Wind waves	Swells
N	0.7%	3.1%	S	2.4%	5.7%
NNE	1.2%	4.3%	SSW	1.5%	6.2%
NE	1.8%	4.5%	SW	0.8%	1.4%
ENE	2.0%	3.2%	WSW	1.3%	1.1%
E	2.0%	4.8%	W	2.8%	2.4%
ESE	3.3%	6.4%	WNW	3.8%	5.5%
SE	5.8%	5.5%	NW	1.6%	3.0%
SSE	4.2%	5.0%	NNW	1.0%	1.7%
Total	36.3%	63.7%	–	–	–

3.3.2 *Correlation Analysis of Spectral Parameters*

Theoretically, the value of ε should be equal to twice ν for a narrow band spectrum (Longuet-Higgins, 1975). The high correlation between ε and ν is found in this study with the value of 0.94 (Fig. 12), while ε calculated by the present fitting formula ($\varepsilon = 1.25\nu^{0.71}$) is smaller than the theoretical one. A good relation is found between ε and the individual wave height and period, $R(H, T)$, with the correlation coefficient of 0.9 (Fig. 13). The relationship between $R(H, T)$ and ε is $R(H, T) = 1.07\varepsilon - 0.124$. Besides, the wave energy is proportional to the square of wave height in theory. There is a high curvilinear relationship between the significant wave height $H_{1/3}$ and the maximum energy spectral density S_{max} (the correlation coefficient is 0.95), and the empirical relation is $S_{max} = 0.89H_{1/3}^{2.37}$, as shown in Fig. 14.

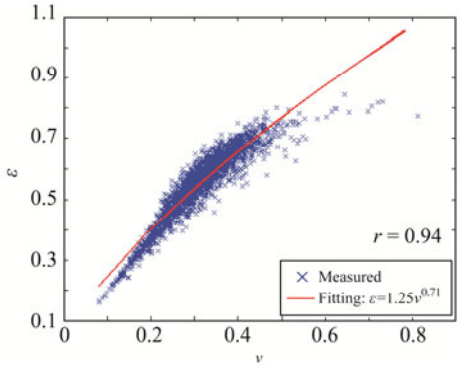

Fig. 12. Variation of ε and ν.

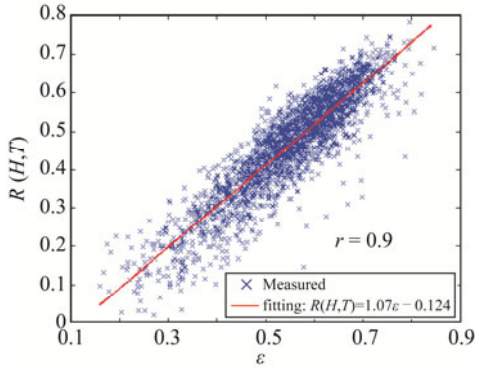

Fig. 13. Variation of $R(H, T)$ with ε.

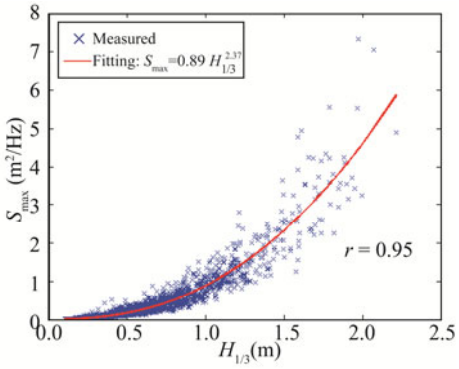

Fig. 14. Relationship between S_{max} and $H_{1/3}$.

3.3.3 *Spectral Analysis*

For the waves at the southern radial sand ridges, the tentative spectral model (Feng *et al.*, 2012) shows a good agreement to the measured spectrum compared with the JONSWAP spectrum (Hasselmann *et al.*, 1973). Thus, this study used the tentative spectral model (TSM), which replaces f^{-5} of high frequency tail with $f_p^{-1}f^{-4}$ to fit the measured spectrum. The formula of TSM is given as follows:

$$S(f)=\frac{\alpha_e g^2}{(2\pi)^4} f_p^{-1} f^{-4} \exp\left[-\frac{5}{4}\left(\frac{f}{f_p}\right)^{-4}\right] \gamma_e^{\exp\left[-\left(\frac{f}{f_p}-1\right)^2 \Big/ 2\sigma^2\right]}, \tag{8}$$

where $S(f)$ is the spectral energy density; α_e is the rear face parameter; γ_e is the peak enhancement factor; g is the gravitational acceleration; f is the wave frequency; f_p is the frequency corresponding to the peak value of energy spectrum; σ is the peak width parameter ($\sigma = 0.07$ for $f \le f_p$; $\sigma = 0.09$ for $f > f_p$).

The tentative spectral parameters α_e and γ_e in Eq. (8), which are calculated by the fitting of $H_{1/3}$ and f_p, can be written as:

$$\alpha_e = 3.368 H_{1/3}^{2.03} f_p^{4.18}; \tag{9}$$

$$\gamma_e = 8.061 H_{1/3}^{0.15} f_p^{0.44}. \tag{10}$$

The corresponding JONSWAP parameters α and γ are:

$$\alpha = 4.069 H_{1/3}^{2.06} f_p^{4.24}; \tag{11}$$

$$\gamma = 6.236 H_{1/3}^{0.12} f_p^{0.34}. \tag{12}$$

In order to analyze the difference between the TSM and JONSWAP model, the spectral peak values, the spectral moments m_0 (zeroth), m_1 (first order), m_2 (second order), are estimated by these two spectral models and compared with the measured spectra. The results are shown in Figs. 15a−15d, respectively. The spectral peak value calculated on the basis of the tentative model is basically consistent with that from the JONSWAP spectrum (Fig. 15a), but the spectral moments m_0 (zeroth order), m_1 (first order), m_2 (second order) calculated by the TSM spectrum are closer to the measured values (Figs. 15b−15d). It means that the TSM spectrum agrees well with the measured spectra rather than the JONSWAP spectrum.

3.4 Wave Groups

Many researchers used the run length (Goda, 1970) as the index in the description of wave group. The run length is defined as the number of continuous waves whose wave heights are more than a certain wave height H_c in the statistical theory of runs. The average value of run lengths in a wave record is defined as the mean run length, and the longest run in a record is defined as the maximum run length and the same to the run length containing H_{max}.

Generally, the large waves are used to estimate the above run parameters. This paper conducts statistical analysis of the run parameters by using the waves with the significant wave height larger than 1 m, and then compares with those at other sea areas (see Table 4). In the present study, the mean run lengths varied from 1.08 to 2.73 with the average of 1.5, the run lengths containing H_{max} varied from 1 to 9 with the average of 2.56 and the longest run length contained 10 waves. Table 4 lists the average values of the mean run lengths, the run lengths containing H_{max} and the maximum run lengths of this study, the Indian Coast (Kumar *et al.*, 2003), the Japanese Coast (Goda, 1976), the West Bohai Sea (Fan *et al.*, 1998), the Jiaozhou Bay (Chang, 1987), and Lianyungang Port (Ge, 1986),

respectively. From Table 4, we can see that, except those at the West Bohai Sea, the run parameters in this study are generally larger than those at other sea areas.

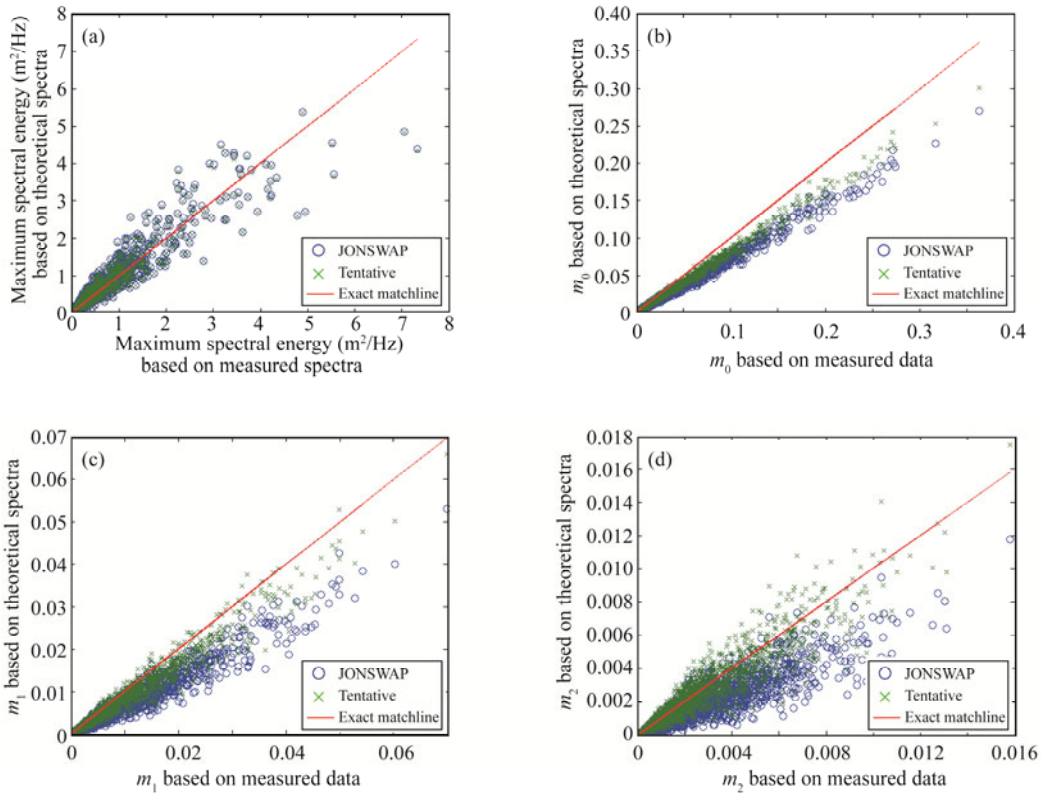

Figs. 15. (a) Scatter plots of the maximum spectral energy based on the measured spectra and that calculated from the TSM spectrum and the JONSWAP spectrum; (b)−(d) Variation of spectral moments based on the measured spectra and that calculated from the TSM spectrum and the JONSWAP spectrum (b) m_0, (c) m_1, (d) m_2. Note: the closer the points are to the match line, the smaller difference between the calculated and measured results.

Table 4 Length parameters of wave group in different sea areas

Sea area	Mean run length	Run length containing H_{max}	Maximum run length	No. of data	Range of data
This study	1.50	2.56	10	298	$H_s > 1.00$ m
Indian Coast	1.36	2.17	9	2661	$H_s > 0.15$ m
	1.32	2.02	8	1943	$H_s > 0.28$ m
	1.28	1.81	7	2476	$H_s > 0.10$ m
	1.33	2.00	7	1682	$H_s > 0.21$ m
Japan Coast	1.42	2.36	7	171	–
West Bohai Sea	1.56	2.03	7	120	$H_{mean} > 0.60$ m
Jiaozhou Bay	1.40	2.29	7	70	$H_s > 0.70$ m
Lianyungang Port	1.41	2.27	8	100	$H_s > 1.00$ m

4. Conclusions

(1) The significant wave height ($H_{1/3}$) varies from 0.15 to 2.22 m with the average of 0.59 m, and the mean wave period (T_{mean}) varies from 2.06 to 6.82 s with the average of 3.71 s during the measurement period.

(2) The wave direction of the highest occurrence is SE with the occurrence of 11.2% in the whole year, while for the waves with $H_{1/3}$ >1 m, the wave direction of the highest occurrence is WNW with the occurrence of 13.2%.

(3) There are significant relationships among the characteristic wave heights, characteristic wave periods and spectral width parameters.

(4) The percentage of single-peaked wave in the wave spectra during the measurement period is 88.6, in which 36.3% of waves are wind waves with high occurrences in the SE, SSE and WNW directions, and the rest are young swells with high occurrences in the WNW, ESE to SSW directions.

(5) The TSM spectrum agrees well with the measured spectra in comparison with the JONSWAP spectrum.

(6) The mean run lengths with the wave height larger than $H_{1/3}$ varies from 1.08 to 2.73 with the average of 1.5, and the run lengths containing H_{max} varies from 1 to 9 with the average of 2.56. The longest run length contains 10 waves. The lengths of the wave group in this study are larger than those of other sea areas.

Acknowledgements — The authors gratefully thank the Research Institute of Coastal and Ocean Engineering, Hohai University, for providing the wave records. They also thank Prof. CHEN Yong-Ping and Mr. CHU Ao for improving the manuscript writing in English.

References

Cartwright, D. E. and Longuet-Higgins, M. S., 1956. The statistical distribution of the maxima of a random function, *Proceedings of the Royal Society of London*, *Series A*, *Mathematical and Physical Sciences*, **237**(1209): 212−232.

Chang, D. F., 1987. Statistical analysis of wave groups in the Jiao Zhou Bay, *Coastal Engineering*, **6**(1): 32−43. (in Chinese)

Ewing, J. A., 1973. Mean length of runs of high waves, *J. Geophys. Res.,* **78**(12): 1933−1936.

Fan, S. T., Wang, Y. M. and Wang, T., 1998. Statistical analysis of wave group in the west of Bohai Sea, *Studia Marina Sinica,* **40**, 13−20. (in Chinese)

Feng, W. B., Yang, B., Cao, H. J. and Ni, X. Y., 2012. Study on wave spectra in south coastal waters of Jiangsu, *Applied Mechanics and Materials,* **212-213**, 193−200.

Feng, W. B., Zhang, Y., Peng, X. L., Zhang, S. L. and Feng, X., 2009. Statistical Study of wind waves for China southern Yellow Sea, *Proceedings of the 5th International Conference on Asian and Pacific Coasts*, 193−200.

Funke, E. R. and Mansard, E. P. D., 1980. On the synthesis of realistic sea state in a laboratory flume, *Proc. 17*th *Int*. *Conf. Coast. Eng*., **1**(17): 2974−2991.

Gao, Z. R., 1995. Analysis of shallow wind-wave distribution and spectrum in Lvsi, *Coastal Engineering*, **14**(2): 1−8. (in Chinese)

Ge, M. D., 1986. On statistical analysis of the grouping waves in Lianyungang, *Journal of Oceanography of Huanghai & Bohai Seas*, **4** (2): 8−14. (in Chinese)

Gluhovskii, B. H., 1968. Distribution characteristics of wave parameters and changes in wave action with depth, Rep. St. Inst. *Oceanology*, **93**, 98−111. (in Russian)

Goda, Y., 1970. Numerical experiments on wave statistics with spectral simulation, *Report of the Port and Harbour Research Institute*, **9**(3): 3−57. (in Japanese)

Goda, Y., 1974. New wave pressure formulae for composite breakwaters, *Proc. 14th Int. Conf. Coast. Eng.*, Copenhagen, Denmark, **1**(14): 1702−1720.

Goda, Y., 1976. On wave groups, *Proceedings Boss*, Trondheim, Norway, **76**(1): 115−128.

Goda, Y., 1979. A review on statistical interpretation of wave data, *Report of the Port and Harbour Research Institute,* **18**, 5−32. (in Japanese)

Goda, Y., 2000. *Random Seas and Design of Maritime Structures*, World Scientific Publishing Co. Pte. Ltd, 268−280.

Goda, Y., 2003. Revisiting Wilson's formulas for simplified wind-wave prediction, *J. Waterw. Port Coast. Ocean Eng.*, ASCE, **129**(2): 93−95.

Hasselmann, K., Barnett, T. P., Bouws, F., Carlson, H., Cartwright, D. E., Enke, K., Ewing, J. A., Gienapp, H., Hasselmann, D. E., Krusemann, P., Meerburg, A., Müller, P., Olbers, D. J., Richter, K., Sell, W. and Walden, H., 1973. Measurements of wind-wave growth and swell decay during the Joint North Sea Wave Project (JONSWAP), *Erganzungsheft zur Deutschen Hydrographischen Zeitschrift*, **A8** (12): 95.

He, X. Y., Hu, T., Wang, Y. P., Zou, X. Q. and Shi, X. Z., 2010. Seasonal distributions of hydrometeor parameters in the offshore sea of Jiangsu, *Marine Sciences*, **34**(9): 44−54. (in Chinese)

Jiangsu Province Resources Survey Leading Group Office, 1996. *Comprehensive Survey of Island Resources in Jiangsu Province*, Scientific and Technical Documents Publishing Office, 80−86. (in Chinese)

Kumar, V. S., Anand, N. M., Kumar, K. A. and Mandal, S., 2003. Multipeakedness and groupiness of shallow water waves along Indian Coast, *J. Coast. Res.*, **19**, 1052−1065.

Kumar, V. S., Johnson, G., Dora, G. U., Chempalayil, S. P., Singh, J. and Pednekar, P., 2012, Variations in nearshore waves along Karnataka, west coast of India, *J. Earth Syst. Sci.*, **121**(2): 393−403.

Kumar, V. S., Philip, S. and Balakrishnan, T. N., 2010. Waves in shallow water off west coast of India during the onset of summer monsoon, *Annales Geophysicae*, **28**(3): 817−824.

Kumar, V. S., Singh, J., Pednekar, P. and Gowthaman, R., 2011. Waves in the nearshore waters of northern Arabian Sea during the summer monsoon, *Ocean Eng.*, **38**, 382−388.

Longuet-Higgins, M. S., 1952. On the statistical distribution of the heights of sea waves, *Journal of Marine Research*, **11**(3): 245−265.

Longuet-Higgins, M. S., 1975. On the joint distribution of the periods and amplitudes of sea waves, *J. Geophys. Res.*, **80**(18): 2688−2693.

Portilla, J., Ocampo-Torres, F. J. and Monbaliu, J., 2009. Spectral partitioning and identification of wind sea and swell, *Journal of Atmospheric and Oceanic Technology*, **26**(1): 117−122.

Suh, K. D., Kwon, H. D. and Lee, D. Y., 2010. Some statistical characteristics of large deepwater waves around the Korean Peninsula, *Coast. Eng.*, **57**(4): 375−384.

U. S. Army Coastal Engineering Research Center (U. S. Army), 1977. *Shore Protection Manual*, 3rd ed., U. S. Government Printing Office, Washington, D.C., USA.

Vandever, J. P., Siegel, E. M., Brubaker, J. M. and Friedrichs, C. T., 2008. Influence of spectral width on wave height parameter estimates in coastal environments, *J. Waterw. Port Coast. Ocean Eng.*, ASCE, **134**(3):187−194.

Yu, Y. X. and Liu, S. X., 1991. The grouping characteristics of sea waves in the Shijiu Port, *Acta Oceanological Sinica*, **10**(3): 451−461.